



International Conference on Sustainable and Intelligent Manufacturing, RESIM 2016, 14-17
December 2016, Leiria, Portugal

Multiscale structure evolution in electrically conductive nanocomposites studied by SAXS

Imran Khan^{a,b}, Saeed D. Mohan^c, Miguel Belbut^a, Christina S. Kamma-Lorger^d, Artur Mateus^a, Geoffrey R. Mitchell^{a*}

^aCentre for Rapid and Sustainable Product Development, Institute Polytechnic Leiria, Marinha Grande 2430-028, Portugal.

^bPhysics Department, Universitat Autònoma de Barcelona, 08193 Bellaterra, Spain.

^cDepartment of Chemistry, University of Reading, Whiteknights, Reading, RG6 6AD, UK.

^dNCD beamline, Alba Synchrotron Light Source, Cerdanyola del Vallès 08290, Spain.

Abstract

The successful introduction of nanostructured materials is hampered by the lack of a quantitative and qualitative understanding of the structure–property relationship within the nanocomposites. Variation in the electrical conductivity of nanocomposite materials depends on the structure evolution of the nanoscale fillers within the polymer phase. This article pertains to the small angle x-ray scattering study of electrically conductive nanocomposites to understand the structure-property relationship. The nanocomposites in this study are comprised of thermoset polyurethane as the matrix material with carbon nanotubes as the filler material. A percolation threshold of 0.5% wt/wt was observed along with substantial changes in the electrical conductivity of the nanocomposites. The small angle x-ray scattering data exhibits mass and surface fractal regimes indicating multiple structure evolution in the nanocomposites. Moreover, the data is interpreted using the crossovers of the scaling laws and sizes are measured to characterize the microstructure with a possible explanation for structural development.

© 2017 Published by Elsevier B.V. This is an open access article under the CC BY-NC-ND license (<http://creativecommons.org/licenses/by-nc-nd/4.0/>).

Peer-review under responsibility of the scientific committee of the International Conference on Sustainable and Intelligent Manufacturing

Keywords: Nanocomposites; carbon nanotubes; electrical conductivity; percolation; structure.

* Corresponding author. Tel.: +351 244 569 441
E-mail address: geoffrey.mitchell@ipleiria.pt

1. Introduction:

Carbon nanotubes (CNT) based nanocomposite materials are high-performance, multifunctional materials with a wide array of promising applications. The networks of carbon nanotubes transfer their unique properties into composite materials to enhance their electrical, electromagnetic [1] and sensor [2] properties through substantial change in the microstructure. As the name suggests, carbon nanotubes are a material comprised of a carbon, whose atoms are arranged in a two-dimensional hexagonal lattice forming a sheet that has been rolled up into a cylindrical structure. The nanotubes can be ten's of nanometres in diameter, however they can possess lengths on the order of micrometres. The nanotubes can exist as a single rolled up sheet referred to as a single wall carbon nanotube, or can be comprised of several sheets forming concentric cylinders, which are referred to as multi-walled carbon nanotubes (MWCNTs). Carbon nanotubes tend to form micron-size aggregates that contain tens to hundreds of nanotubes. These MWCNTs do not disperse easily and tend to agglomerate in polymer matrices due to high surface area and strong Van der Waal forces between themselves [3]. The literature suggests that different organic/inorganic solvents can be used to aid in the dispersion of CNTs in order to achieve an adequate CNT-CNT network morphology, however, colloidal stability is far from ideal and can lead to aggregation and agglomeration during the formulation process of the nanocomposites. Such processes lead to the development of a complex morphology, which can make an interesting area of study to examine the particulars of this complex structure resulting from the filler loading. Expanding on the knowledge of how these complex structures form and potentially lead to develop and design of composites with enhanced electrical conductivity.

Small angle x-ray scattering (SAXS) is a useful technique to study microstructure in nanocomposites. Contrary to a lot of literature available on structural and morphological analysis of nanocomposites using SAXS, filler concentration dependent structural evolution and development contributing to conductivity enhancement still demands a thorough analysis. It had been observed that for SAXS data on samples containing carbon nanotubes with ≤ 0.05 %wt a simplified tube form factor (STFF) scattering model can be applied to the data, however, at higher loadings of CNT filler, the STFF fails to account for the excess scattering at low scattering angles [4]. The excess scattering at the low scattering angles has been attributed to the development of an entangled network of semi flexible nanotubes for concentrations more than 0.05% [5]. As the concentration of the filler increases the CNTs are no longer isolated from one another, hence the scattering observed is no longer the result of individual isolated tubes, but also the scattering correlated between the neighbouring particles. CNT networks have been observed to contain micron size aggregates with some distributions in their size [6]. Aurilia et al. reported that nanotubes modify thermoset polyurethane micro domain morphology and their state of aggregation varies with their type [7]. The large scale aggregates and micro domain morphologies developed become important considerations for future developments of nanocomposite materials. Therefore an understanding of how these structures develop with increasing filler concentration becomes an important factor. This work is a contribution to understanding the complex structures caused by MWCNTs networks in electrically conductive nanocomposites through use of SAXS.

2. Materials and Methods:

Multiwall carbon nanotubes (MWCNTs), having 3 to 6 walls, were purchased from Sigma-Aldrich, Portugal. Two part thermoset polyurethane (TSPU) is obtained from Huntsman group, Germany. Part A was an industrial grade polyol containing the blend of hydroxyl groups containing light hydro treated petroleum distillates. Part B was a diphenylmethane diisocyanate (MDI). DMF (N, N Dimethylformamide) is obtained from Merck, Germany. MWCNTs were dispersed in DMF using an ultrasonic bath followed by mixing with polyol for 30 minutes. Further, the mixture was kept in a heating chamber at 120°C for 5min followed by vacuum degassing to remove DMF from the mixture. The polyurethane nanocomposites were prepared, after removing DMF from the sonicated mixture, with the addition of an isocyanate into the MWCNT/DMF/polyol mixture with 1:1. A copper mould was used to prepare nanocomposites samples using a hot compression at 120°C for 60 ± 5 seconds. Samples were prepared with filler concentrations of 0.5%, 1%, 1.5%, 2%, 3% and 5% wt/wt. A home built four probe electrical conductivity measurement system was used to measure the electrical conductivity of the nanocomposites. Small angle X-ray scattering (SAXS) was performed on beam line BL11-NCD at ALBA Synchrotron Radiation facility, Barcelona,

Spain. An approximate sample-to-detector distance 6.20m was used with an X-rays beam with $\lambda=0.99 \text{ \AA}$, providing a q range of 0.15 \AA^{-1} where $q=4\pi\sin\theta/\lambda$, and 2θ is the scattering angle.

3. Results and discussion:

3.1. Electrical conductivity measurement:

Electrical conductivity measurements of the prepared samples show a transition from insulator to a conductor at the loading of 0.5% wt/wt MWCNTs with electrical conductivity reaching $2.1 \times 10^{-4} \text{ s/m}$. This is considered as a transition concentration (ϕ_o) for the nanocomposite as shown in figure 1. Some studies suggests MWCNTs have required loadings at up to 5–10 wt% to obtain similar conductivity values [1]. The maximum measured electrical conductivity (σ_{max}) of nanocomposites in this study was $2.2 \times 10^{-1} \text{ s/m}$, measured for the sample containing the highest loading of MWCNTs at 5% wt/wt. The MWCNT/polyurethane nanocomposite films showed conductivities of several orders of magnitude higher than the conductivities of neat polyurethane as shown in Fig. 1. The dramatic increase in electrical conductivity relates to electrical pathway development from the formation of MWCNTs networks. The formation of MWCNTs network or a continuous electron path is the main cause of the electron transport by tunneling or electron hopping which occurs along MWCNT interconnects. When the percolation threshold is reached, the formation of a percolated filler network structure, where a critical minimum distance between MWCNTs structures has been attained and electron conduction is facilitated through a ‘hopping’ or ‘tunnelling’ mechanism[8]. Fig. 1 provides a plot of the MWCNT loading in the nanocomposite materials vs. the electrical conductivity. From the data shown in Figure 1 we can see that 3 regimes are present: (1) insulator or dielectric ($\phi < \phi_o$), (2) transition ($\phi \approx \phi_o$) and (3) metallic or conductor ($\phi > \phi_o$).

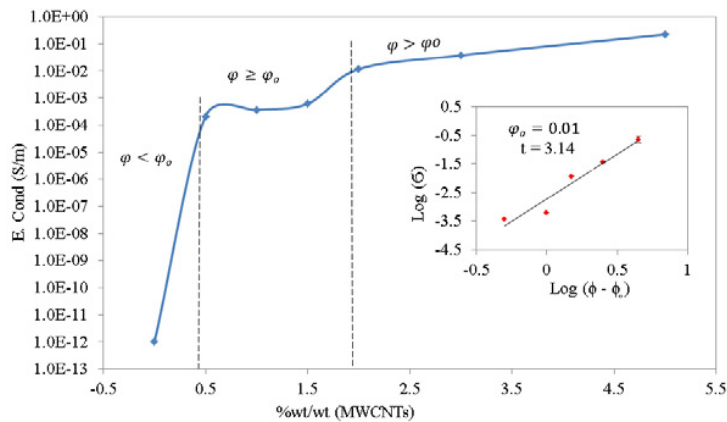


Fig. 1. Plot of % content of MWCNT (ϕ) versus Log of electrical conductivity. Inset shows electrical conductivity data fit using Equation (1). The error bars represent the 2 standard deviations for three samples per composition.

The concentration dependent increase in electrical conductivity is explained with the help of percolation theory, Equation (1) [9]:

$$\sigma(\phi) = \sigma_o (\phi - \phi_o)^t, \phi > \phi_o \tag{1}$$

where t is the critical exponent, ϕ is the weight fraction of multiwall carbon nanotubes, ϕ_o is the percolation threshold or the minimum carbon nanotubes concentration for transition from insulator to conductor state, and σ_o represents electrical conductivity of carbon nanotubes. Further, a double logarithmic plot is used to extract the magnitude of the critical exponent from experimental data using Equation (1) (Fig. 1 inset), for which a value of $t = 3.1$ is obtained. Here the best fitting is characterized by the correlation coefficient, R^2 for which a best possible fit $R^2 = 1$. For the data inset in Fig. 1 a value of $R^2 = 0.94$ was obtained. The measured value of the critical exponent is relatively high compared to theoretical values predicted [10], however, it is comparable to the values reported in the

literature for other polymer nanocomposites [11, 12]. The value obtained for the critical exponent in different studies ranges between 1.6 [13] and 2 [14] for networks of filler in a polymer matrix. The deviation of the critical exponent can be attributed to a number of parameters e.g. the composition of the composite system, the type of the conduction mechanism, the difference between a perfect lattice of inclusions and a real polymer–particles system (orientation, aspect ratio), the degree of dispersion of the filler, the method of fabrication etc. Polymer matrix kinetics and interactions between phases as well as between conductive particles are some of the reasons that constitute this discrepancy in the critical exponent [15, 16, 17].

3.2 Small angle X-ray scattering:

Fig. 2 shows the SAXS scattering intensity as a function of the modulus of scattering vector (q) on a log-log plot for the TSPU/MWCNT nanocomposites for all concentrations studied. A gradient -4.3 is measured for the neat thermostat (TSPU) polyurethane while the nanocomposite materials exhibit more than one gradient present in the scattering curves. Four different gradients were observed in the nanocomposites, which became more prominent at higher MWCNT loadings. Fig. 2a shows the regions are differentiated from each other on the basis of variation in gradient and marked as Region-I, Region-II, Region-III and Region-IV for the respective q - ranges: $q_1 \rightarrow 0.0044-0.022$, $q_2 \rightarrow 0.022-0.048$, $q_3 \rightarrow 0.048-0.083$ and $q_4 \rightarrow 0.083-0.12$ as shown in Fig.2 (b to e).

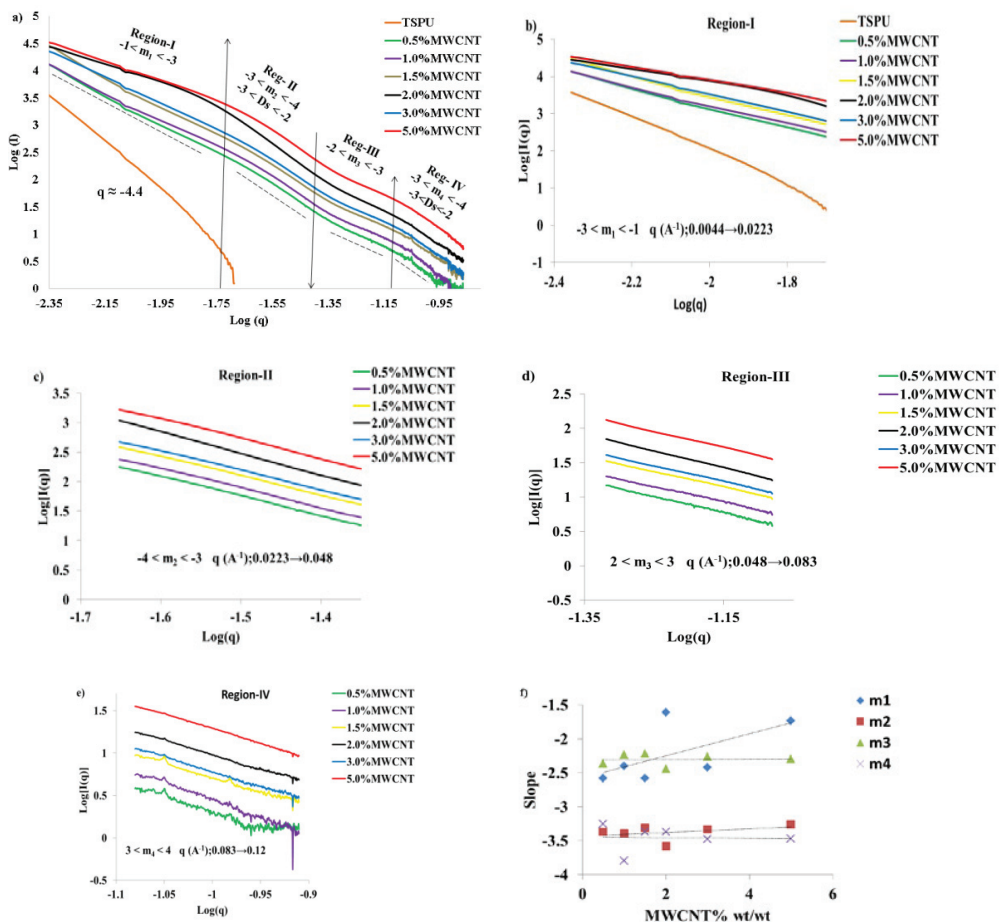


Fig. 2. (a); Slopes obtained from log-log plots of $I(q)$ as a function of q for TSPU/MWCNT nanocomposites with different % (wt/wt) MWCNTs. The gradients are denoted as m_1, m_2, m_3 and m_4 in the respective four regions. b to e) four regions with different gradients. f) Variation in gradients as measured from plots b to e under the effect of MWCNTs %wt loading.

Two features are apparent for the data with regards to increases in concentration of carbon nanotubes; 1) A change in gradient in double logarithmic plot of q vs. $I(q)$ for all concentrations observed, as compared to neat polyurethane (Fig. 2 (a)). The transition points for the power laws became prominent at relatively higher MWCNT loading (2% and 5%) with the exception of 3%. The gradients, here in and afterwards, from Region-I to a Region-IV are denoted as m_1, m_2, m_3 and m_4 , respectively. The gradients obtained from these regions correspond to either the mass fractal or surface fractal morphology. Specifically, the gradients obtained from Region-I and Region-III were $-3 < m_1 < -1$ and $-3 < m_3 < -2$, respectively, indicating mass fractal morphology of the nanocomposite. Further, in Region-I, a transition in mass fractal dimension was observed from $-3 < m_1 < -2$ to $-2 < m_1 < -1$ with MWCNTs loading (2.0%wt and 5.0%). The mass fractal dimension slightly varies in Region-III and remained within the limit $-3 < m_3 < -2$ for all carbon nanotubes concentrations. The gradients in Region-II and Region-IV are $-4 < (m_i)_{i=2}, 4 < -3$, characteristic of fractal surfaces with fractal dimension $2 < D_s < 3$.

The form factor for cylinders shows a low- q part which varies as $1/q^1$ and a high- q part that dies out as $1/q^4$ indicating sharp interfaces or a smooth surface. Region-I and Region-IV are the respective low q and high q parts of the plots shown in Fig. 2(a). The absence of $1/q^1$ in Region-I is an indication that MWCNTs form clusters or aggregate leading to develop fractal morphology in the nanocomposites. The variation in gradients with carbon nanotubes %wt is shown in Fig. 2(e).

Table1: Approximate agglomerate size measured using correlation length (ξ) for nanocomposites containing 0.5%wt/wt MWCNTs.

q-range (Å)	$D=2\pi/q$ (Å)	Nature of cross-over point	Structure
0.0197	318.7	Inter-cluster	aggregate
0.0500	125.6	Intra- cluster	branch
0.0850	71.6	Porod scattering	Surface

The range of fractal behaviour could be defined by $\xi^{-1} < q < l^{-1}$, where ξ^{-1} is the upper bound limit used to represent the size of the aggregate or cluster and the lower limit l^{-1} represents the size of individual carbon nanotubes constituting the aggregates. The values for upper and lower bound limits can be deduced using $D=2\pi/q_{\min}(q_{\max})$, where q_{\min} and q_{\max} represents the upper and lower bounds respectively. The meaning of ξ is only qualitative and has to be made precise in any particular situation. Generally, the correlation length (ξ) represents the characteristic distance above which the mass distribution in the sample is no longer described by the fractal law [18]. In practice, it can represent the size of an aggregate or a correlation length in a disordered material [19]. ξ was measured using the crossover points differentiating the fractal regimes to measure size of the aggregate in the nanocomposite material [19] (Table 1). Fig. 3 shows a visual representation of the crossover points differentiating the fractal regimes transition from a large-scale network to internal branched structures. Such transitions can be located at the intersection of the power-laws describing the low- q and the intermediate- q scattering.

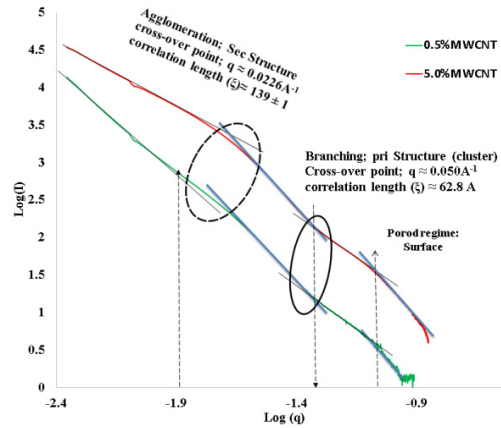


Fig.3. Log-log plot for 0.5% and 5.0% TSPU/ MWCNT nanocomposites. The cross-over points indicates correlation length for aggregates and branch structures in the nanocomposites.

An estimate of the radius of gyration (R_G) is obtained using mass fractals and ζ [19] and is calculated using Equation (2).

$$R_G^2 = \frac{D_m(D_m+1)\zeta^2}{2} \text{ for } -3 < D_m < -1 \quad (2)$$

The results of ζ and R_G obtained from the analysis are tabulated in Table 2. Both ζ and R_G were observed to decrease with MWCNTs loadings in Region-I without any significant change in Region-III. It indicates that structure develops in Region-I with %wt of MWCNT without altering structure in Region-III.

Table 2: Parameters extracted using Equation (2) from Region-I and Region-III is shown in Figure 2(a).

Region	%MWCNT (ϕ)	Crossover point (q) (\AA^{-1})	Corr. length (ξ) (\AA)	Mass fractal dim. (D_m)	Radius of gyr. (R_G) (\AA)
Region-I	0.5	0.0031	322.5	-2.7	488.5
	1.0	0.0031	322.5	-2.5	441.6
	1.5	0.0038	263.1	-2.6	379.4
	2.0	0.0035	285.6	-1.8	242.4
	3.0	0.0034	294.0	-2.4	381.1
	5.0	0.0036	277.7	-1.8	235.6
Region-III	0.5	0.0458	21.8	-2.36	27.7
	1.0	0.0446	22.4	-2.23	26.3
	1.5	0.0461	21.7	-2.22	25.2
	2.0	0.0459	21.8	-2.44	28.9
	3.0	0.0429	23.3	-2.26	27.8
	5.0	0.0464	21.6	-2.3	26.4

The Guinier equation (Equation 3) was fitted to few data points near beam stop position in a short q -range. The R_G is calculated from the slopes in the linear fit of $\ln I(q)$ vs. q^2 using Equation 4.

$$I(q) \propto \exp^{-q^2 R_G^2 / 3}, q R_G \leq 1.3 \quad (3)$$

$$R_G = \sqrt{3m} \quad (4)$$

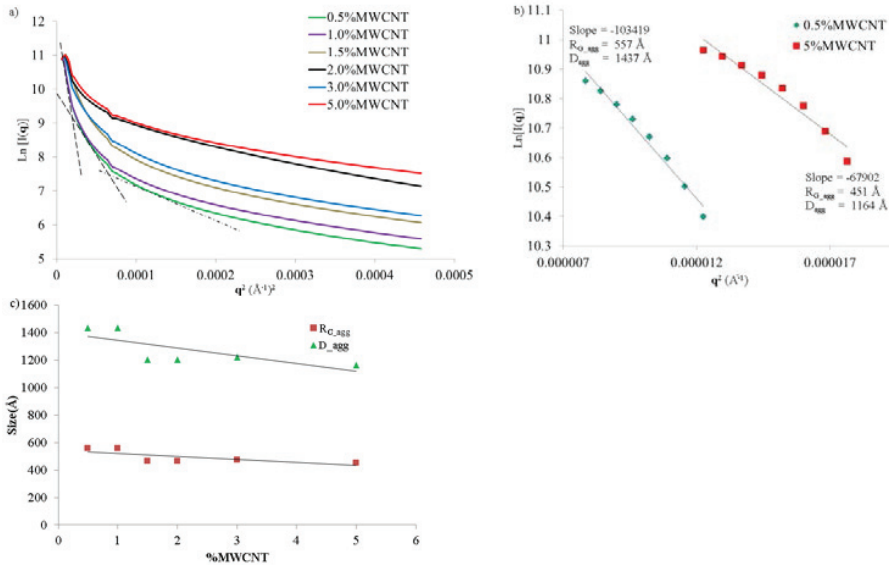


Fig.4. Guinier plot of SAXS intensity decay. a) The non-linear region over the low q regime indicates aggregation of MWCNTs. b) Variation in the radius of gyration (R_G) and respective aggregate size (D_{agg}) for 0.5% and 5.0% carbon nanotubes. c) The solid lines are drawn to show the general trend in R_G and $D_{agglomerate}$ with carbon nanotubes loading.

Analysis of the data using Guinier plots show a curved region (Fig. 4 (a)) contrary to a linear region caused for monodisperse scattering system. This curved region can be attributed to the aggregation of carbon nanotubes. The dotted lines in Fig. 4(a) are used to represent multi-structure in the nanocomposites. The Guinier region shrinks further towards the low q region at relatively higher carbon nanotubes loading making analysis difficult. The results obtained through this analysis for R_G under different carbon nanotube loadings are tabulated in Table 3. A declining trend is observed in the radius of gyration with carbon nanotubes loadings as shown in Fig. 4(b, c). The aggregate shrinks or becomes compact by about 20% as MWCNTS increased 10 times relative to percolation threshold concentration.

The aggregate size corresponding to the radius of gyration was calculated using Equation 5 with the assumption of globular shape of aggregates.

$$R_{agg} = R_{G-agg} / \sqrt{(3/5)} \tag{5}$$

Table 3: Variation in R_G derived from fitting of Guinier law in the limit $0.002801 < q < 0.004201$ and corresponding agglomerate size with % content of MWCNT.

%MWCNT	R_{G-agg} (Å)	R_{agg} (Å)	D_{agg} (Å)
0.5	367.1	473.9	947.8
1.0	366.9	473.7	947.4
1.5	307.4	396.8	793.7
2.0	307.8	397.4	794.8
3.0	312.4	403.37	806.7
5.0	297.4	384.0	768

Kratky-plots can be used to find breaks in the slope corresponding to recognizable maxima [20]. Such maxima correspond to aggregate sizes (q_{agg}) of MWCNTs into the nanocomposite. Two peaks are observed in the Kratky plots, a narrow peak and a broad peak as shown in Fig. 5(a). Absence of a single peak is an indication of multiple peaks containing different populations of aggregates. The Kratky plots follow a Gaussian distribution with two peaks as shown in Fig. 5(b). The green and blue plots fit Kratky data independently indicating existence of two different kinds of structures.

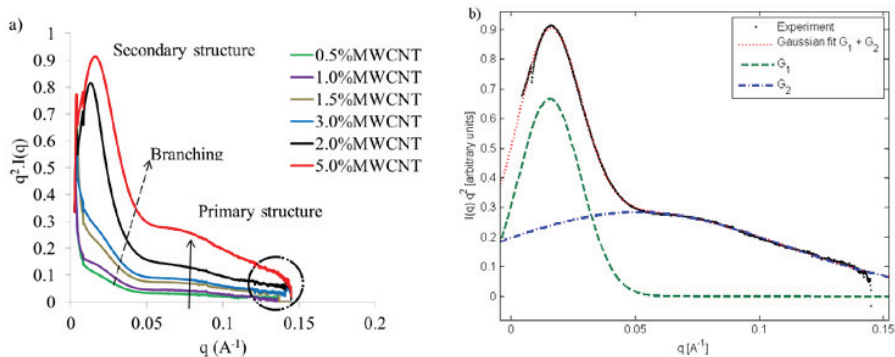


Fig.5. Kratky plots: a) Kratky plots of nanocomposites with different %wt of MWCNTs. b) Two different populations of structures develop with carbon nanotube loading.

The variation in aggregate size with MWCNTs % loading is tabulated in Table 4. The data show the size of aggregates shrink with carbon nanotubes %wt, suggesting that the structure is getting densely packed and compact at relatively higher carbon nanotube loading. Possibly, this is caused by increased attractive forces (Van der Waals) exists between neighbouring MWCNTs. The comparison of R_{agg} suggests that at higher loadings (0.14%vol/wt MWCNTs) the structure become compact $\sim 1/5$ th relative to the structure at percolation threshold.

Table 4: Aggregate size measurement using Kratky plots with different % MWCNTs.

%MWCNT	$q_{agg} (\text{Å}^{-1})$	$R_{agg} = \pi/q_{agg} (\text{Å})$
0.5	0.0029	1083.3
1	0.0029	1083.3
1.5	0.0030	1047.2
2	0.0037	849.1
3	0.0109	288.2
5	0.0156	201.4

Well-defined plateaus are evident at approximately $q = 0.0257 \text{ Å}^{-1}$ and $q = 0.087 \text{ Å}^{-1}$ in the Porod plots as shown in Fig. 6(a). The position of the low- q plateau slightly changed depending on % content of MWCNTs without any significant change in position for high - q plateau. The highest plateau (large dotted circle in Fig. 6(a)) reflects the presence of carbon nanotubes displaying high specific surface areas.

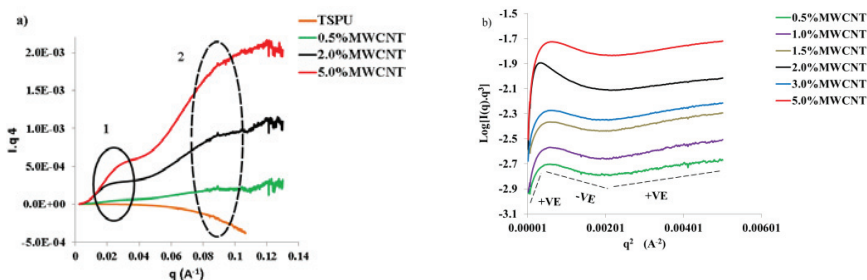


Fig. 6. a) Porod plots. Circles are drawn to show distinct plateaus indicating the specific surface areas of multi-structure aggregates of carbon nanotubes. b) Plots used to indicate deviation from standard Porod’s law due to the presence of either diffuse interface or inhomogeneous electron density.

The presence of another plateau located at lower q (small dotted circle in Fig. 6(a)) indicates that carbon is arranged in secondary structures of finite size, under the assumption that no major contamination of scattering impurity is present. Moreover, the low- q plateau seems to have a similar secondary structure with a different nanotube number density (in terms of cross section and number of walls) [21]. It is important to note that there is no significant difference in terms of position of plateau 2 with MWCNTs %wt while plateau 1 moves up revealing relatively more scattering (21). This indicates that number density of carbon nanotubes and hence the network density increases with increasing MWCNTs %wt, leading to increases multiple paths for electronic conduction in the nanocomposites.

It is evident from the Porod plots that there exists a rough surface within the nanocomposites. The substantial change in surface features can be caused by a number of factors, for example, the presence of diffuse interfaces or electron density inhomogeneity within the structure. This is explored further using Porod law for non-ideal two-phase system as shown in Fig. 6(b). A negative deviation from Porod's law is a characteristic of non-ideal two-phase system with a diffuse interface layer between the carbon nanotubes and polyurethane matrix [22, 23]. The positive deviation is characteristic of a two-phase system with electron density inhomogeneity [22, 23] in the particles. The dotted lines are drawn to distinguish deviations occurred in the experimental plots in Fig. 6(b).

4. Model

It is evident from the SAXS analysis that the structure of nanocomposite is composed of multiple fractal aggregates of carbon nanotubes. It has been known for a long time in the field of carbon-black polymer composites that some level of aggregation favours the formation of a conducting network by decreasing the percolation threshold [16, 24]. It is evident from the SAXS data analysis that MWCNTs causes to evolve two mass fractal morphologies in the nanocomposites. The mass fractal morphology in the low- q region (Region-I in Fig. 2) further changes with MWCNTs loading and transform into compact and densely packed aggregates of carbon nanotubes while the mass fractal morphology in intermediate q -region (Region-III in Fig. 2) does not change significantly indicating a sparsely structure contain few tubes in the intermediate q -region. The compact, dense structure is somewhat similar to packing density that defines the degree of contact between the carbon nanotubes within the aggregate. The sparsely structures contain few MWCNTs connect the aggregates of MWCNTs. It is important to emphasize at this point that a full dispersion of MWCNT network may be considered undesirable for electrical conductivity enhancement, rather, inhomogeneous microstructure consisting of non-dispersed MWCNT (aggregates) bridged by dangling chains (clusters) tend to result in higher DC conductivity [25]. The discussion can be summarized in a brief model to depict possible network development in the nanocomposite as shown in Fig.7.

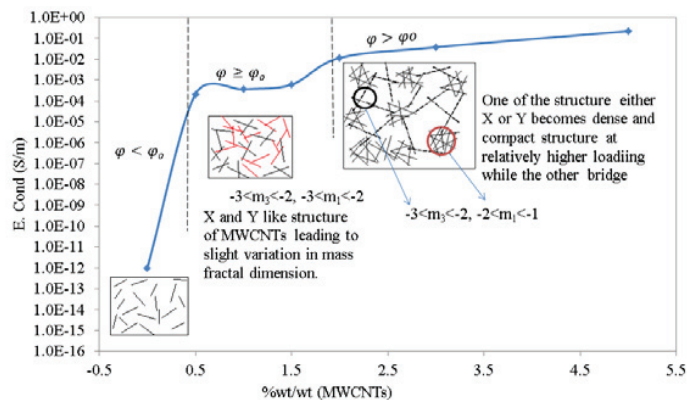


Fig.7: Possible network evolution model causes to increase electrical conductivity in the nanocomposite with the relative increase in MWCNTs.

Conclusion:

Small angle x-ray scattering study was conducted to understand network morphology of multiwall carbon nanotubes into a thermoset polyurethane matrix. The presence of the carbon nanotubes caused an increase in electrical conductivity, rising with increasing loadings in the nanocomposites for the samples examined. Examination of the nanocomposite materials revealed that the presence of the carbon nanotubes causes a multifractal morphology to develop. A transition in mass fractal morphology was observed, which becomes prominent at relatively higher carbon nanotubes loading. The transition between different scaling regimes used to identify the characteristic size scale of fractal aggregates show the structures becomes compact and dense at relatively higher MWCNT %wt. Moreover, there exists a rough interface between the polymer and MWCNT. The

data suggest two different size scales for the developed structures. The results also indicate that fractal concepts are useful to interpret the complex morphology in nanocomposites containing nanostructure reinforcement. It is concluded that deviations from the universal value for critical exponent “ t ” can be attributed due to the inhomogeneous or multiple level structure development in real nanocomposites compare to ideal or perfect lattice used in classical percolation theory.

Acknowledgements:

This research work was supported by the Portuguese Foundation for Science and Technology (FCT) through the project reference UID/Multi/04044/2013. These experiments were performed at the BL11 beamline at the Alba Synchrotron.

References:

- [1] A.S. Hoang, Electrical conductivity and electromagnetic interference shielding characteristics of multiwalled carbon nanotube filled polyurethane composite films, *Adv. Nat. Sci.: Nanosci. Nanotech.* 2 (2011) 025007 (5pages).
- [2] E.T. Thostenson, T.W. Chou, Carbon nanotube networks: Sensing of distributed strain and damage for life prediction and self-healing, *Adv. Mat.* 18(22) (2006) 2837-2841.
- [3] M. Shifa, F. Tariq, K. Ali, R.A. Baloch, Effect of aryl diazonium salt functionalization on the electrical properties of MWCNTs and MWCNTs/CF reinforced polymer composite, *Int. Conf. Aer. Sci. Eng.* 4th (2015) Pakistan.
- [4] R.S. Justice, D.H. Wang, L.S. Tan, D.W. Schaefer, Simplified tube form factor for analysis of small-angle scattering data from carbon nanotube filled systems, *J. App. Cry.* 40 (2007) s88-s92.
- [5] D.W. Schaefer, R.S. Justice, How nano are nanocomposites, *Macromolecules* 40 (2007) 8501-8517.
- [6] I. Khan, G.R. Mitchell, A. Mateus, C.S.K. Lorgier, Time resolved strain dependent morphological study of electrically conducting nanocomposites, *J. Phy. Conf. Ser.* 646 (2015) 4pages.
- [7] M. Aurilia, M. Lavorgna, L. Sorrentino, S. Iannace, E. Milella, MWCNTs for tuning viscoelastic and inelastic properties of elastomeric materials, 15th Eur. Conf. Comp. Mat. (2012) 8pages.
- [8] C. Min, X. Shen, Z. Shi, L. Chen, Z. Xu, The electrical properties and conducting mechanisms of carbon nanotube/polymer nanocomposites: a review, *Pol.-Plas Tech. Eng.* 49 (2010) 1172–1181.
- [9] S. Kirkpatrick, Percolation and Conduction, *Rev. Mod. Phys.* 45 (1973) 574-588.
- [10] D. Stauffer, Introduction to percolation theory, 1st ed., Taylor & Francis, London and Philadelphia, 1985.
- [11] A. Vavouliotis, E. Fiamgou, P. Karapappas, G. Psarras, V. Kostopoulos, Electrically conductive epoxies using multiwall carbon nanotubes, *Soc. Pl. Eng.*, DOI: 10.2417/spepro.002915, 2010.
- [12] O. Kanoun, C. Müller, A. Benchirouf, A. Sanli, T.N. Dinh, A. Al-Hamry, L. Bu, C. Gerlach, A. Bouhamed, Flexible carbon nanotube films for high performance strain sensors, *Sensors* 14 (2014) 10042-10071.
- [13] S. Kirkpatrick, Percolation and conduction, *Reviews of Modern Physics*, 45(4), 574-588, 1973.
- [14] M.S. Vionnet, C. Grimaldi, T. Maeder, S. Strässler, P. Ryser, Tunneling-percolation origin of nonuniversality: Theory and experiments, *Phy. Rev. B* 71 (2005) 064201- 064212.
- [15] I. Balberg, A comprehensive picture of the electrical phenomena in carbon black-polymer composites, *Carbon* 40 (2002) 139-143.
- [16] S. Barrau, P. Demont, A. Peigney, C. Laurent, C. Lacabanne, DC and AC conductivity of carbon nanotubes-polyepoxy composites, *Macromolecules* 36 (2003) 5187-5194.
- [17] M.T. Connor, S. Roy, T.A. Ezguerra, F.Z.B. Calleja, Broadband ac conductivity of conductor-polymer composites, *Phy. Rev. B* 57 (1998) 2286–2294.
- [18] E. A. Odo, D.T. Britton, G. G. Gonfa, M. Harting, *Int. Jour. Comp. Mat.* 5 (2015) 65-70.
- [19] J. Teixeira, Small-angle scattering by fractal systems, *J. Appl. Cry.* 21(1988) 781-785.
- [20] G.P. Baeza, A.C. Genix, C. Degrandcourt, L. Petitjean, J. Gummel, M. Couty, J. Oberdisse, Multiscale filler structure in simplified industrial nanocomposite silica/SBR systems studied by SAXS and TEM, *Macromolecules* 46 (2013) 317-329.
- [21] K. Rasmussen, J. Mast, P.J.D. Temmerman, E. Verleysen, N. Waegeneers, F.V. Steen, J.C. Pizzolon, Multi-walled carbon nanotubes: Characterisation and physico-chemical properties, European Union, Luxembourg, 2014.
- [22] R. Zhang, Y.X.Q. Meng, L. Zhan, K. Li, D. Wu, L. Ling, J. Wang, H. Zhao, B. Dong, Small angle X-ray scattering study of microstructure changes of organic hydrogels from supercritical carbon dioxide drying, *J. Super. Flu.* 28 (2004) 263-276.
- [23] S. Pikus, E. Kobylas, SAXS studies of porous materials coated by organic layer, *Fib. Text. East. Eu.* 11(2003) 70-74.
- [24] K.E. Sichel, Carbon black-polymer Composites, Marcel Dekker, New York, 1982.
- [25] Y.Y. Huang, E.M. Terentjev, Dispersion of carbon nanotubes: Mixing, sonication, stabilization, and composite Properties, *Polymers* 4 (2012) 275-295.